A Comparative Study of Arc Behavior in an Auto-expansion Circuit Breaker with Different Arc Durations

[1]Y Pei, [2]J Zhong, [3]J Zhang and[4]J D Yan

[1,4]Department of Electrical Engineering and Electronics, University of Liverpool, Brownlow Hill, Liverpool L69 3GJ, UK

[2]R&D Centre, Pinggao Group Co. Ltd, 22 Nanhuandonglu Road, Pingdingshan City, Henan Province, 467001, China

[3]School of Automatic Science and Electrical Engineering, Beihang University, Beijing, 100191, China

Email: yuqing@liv.ac.uk, zhongjy@pinggao.sgcc.com.cn, jmzhang@buaa.edu.cn and yaneee@liv.ac.uk

Abstract. A computational study of the thermal interruption performance of a 145 kV, 60 Hz auto-expansion circuit breaker has been carried out. The pressure peak in the expansion volume has a delay of 2.8 - 3.4 ms with reference to the current peak when the arc duration varies. A reasonable indicator of the interruption environment is the average mass flux in the main nozzle. The short arc duration case (12.25 ms) is the most difficult case with the lowest critical rate of rise of recovery voltage (RRRV) of 10 kV/μs, just above the initial system applied RRRV of 9 kV/μs. This is a result of insufficient gas flow cross sectional area between the live contact and the main nozzle to develop rapid gas flow for arc cooling. The auxiliary nozzle plays two roles. It provides blockage in the high current phase to reduce gas exhaustion from the main nozzle into the hollow contact; after current zero the hollow contact shares a considerable portion of the system recovery voltage, especially for the short arc duration case (36%). Therefore the proper design and use of an auxiliary nozzle is key to enhancing the thermal interruption capability of high voltage auto-expansion circuit breakers.

1. Introduction

Auto-expansion (self-blast) circuit breakers [1] are advantageous over puffer type gas circuit breakers (GCBs) [2][3] in that the former utilizes the energy of the arc to build up a high pressure reservoir in the high current phase which develops and maintains high speed gas flow in the nozzles during the current zero period to cool and quench the arc. The driving energy of an auto-expansion circuit breaker is thus considerably lower than that of a puffer circuit breaker of the same switching ratings. In comparison with a puffer circuit breaker, an auto-expansion circuit breaker has much more complex interruption behaviour with different arc durations because of the fact that pressure build-up in the expansion volume (or heating chamber) depends on the arc's history [1].

A well-designed circuit breaker should ensure that the arc is always successfully quenched with the live contact being at all its possible positions between the shortest and longest permitted arc durations. The shortest arc duration is normally found in type tests with a pre-defined procedure. With different arc

durations the live contact is at different axial positions (different contact gap lengths) when the current passes its final zero point and a recovery voltage is subsequently applied. Variation in arc duration has two important implications. Firstly, the relevant position of the live contact tip in the main PTFE nozzle will determine the nozzle surface area that is exposed to arc radiation around the current peak(s) and subsequently the amount of PFFE vapour produced in the high current phase for pressurisation of the expansion volume. Secondly, the position of the live contact tip may affect the effective gas flow cross sectional area through the main nozzle and thus the development of flow field around the arc column at current zero, directly affecting the interruption capability of the breaker. The influence of arc duration on the interruption capability of auto-expansion circuit breakers has so far not been studied in details by computer simulation, as a result of long computational time and the availability of reliable arc models.

This paper presents a comparative study of the arcing process in a 145 kV auto-expansion circuit breaker with different arc durations by using a newly developed automated simulation platform, the Integrated Simulation and Evaluation Environment (ISEE) [4]. Analysis has been carried out through detailed energy balance, enthalpy flow rate, and distribution of temperature and flow fields at key instants to explain the relationship between the predicted critical rate of rise of recovery voltage (RRRV) of the breaker and the arc durations, using sinusoidal short circuit current waveforms and an identical contact travel curve. Information from this work is expected to be of interest to high voltage circuit breaker designers. Important details of the arc model are given in Section 2 and results presented and analysed in Section 3. Conclusions are drawn in Section 4.

2. The arc model

The arc together with its surrounding gas flow is assumed to be axis-symmetric and in local thermodynamic equilibrium (LTE) state. The problem can be mathematically described by time-averaged Navier-Stokes equations taking account of Ohmic heating, electromagnetic effect (Lorenz force), nozzle ablation, radiation loss and turbulence enhanced mass, momentum and energy transport. The general conservation equations in a 2D cylindrical coordinates can be written in the follow form:

$$\frac{\partial(\rho\emptyset)}{\partial t} + \nabla \cdot \left(\rho\emptyset\vec{V}\right) - \nabla \cdot (\Gamma_\emptyset\nabla\emptyset) = S_\emptyset \tag{1}$$

where ϕ is the variable to be solved and, ρ and $\vec{V}$ the density and velocity of the gas, respectively. The source term S_Φ and the diffusion coefficient Γ_Φ are listed in Table I, where all notations have their conventional meaning [1].

Table 1. Terms of governing equations.

Equation	ϕ	Γ_ϕ	S_ϕ
Continuity	1	0	0
z-momentum	w	$\mu_l + \mu_t$	$-\partial P/\partial z + J_r B_\theta +$ viscous terms
r-momentum	v	$\mu_l + \mu_t$	$-\partial P/\partial r - J_z B_\theta +$ viscous terms
Enthalpy	h	$(k_l+k_t)/c_p$	$\sigma E^2 - q + dP/dt +$ viscous dissipation
PTFE mass concentration	c_m	$\rho(D_l+D_t)$	0

The equation of state and the thermodynamic and transport properties of SF_6-PTFE gas mixture are given in [5]. A semi-empirical radiation transport model of Zhang et al [6] is used, which assumes a monotonic radial temperature profile with maximum temperature of T_m on the axis. The radiation emission region is defined as that from the axis to the isotherm of $0.83T_m$ (the arc core). The net radiation loss, q, in Table 1 is calculated based on the net emission coefficient (NEC), which is a function of pressure, temperature

and arc radius [7]. High temperature SF_6 gas and PTFE vapour both contain a significant proportion of fluorine element and their NECs are very close to each other for radiation radius larger than 1 mm [8]. For example at a pressure of 4 MPa, which is typical for circuit breaker arcs, the difference between the NECs of SF_6 and PTFE vapour is less than 20% for radiation radius between 1 mm and 10 mm. For computational efficiency, the NEC data of SF_6 is used in the present work.

Experience shows that to make reasonable temperature prediction at the arc centre, the NEC data from Lowke [7] has to be used with a specific definition of the radiation radius. For auto-expansion circuit breakers, the radial temperature profile varies substantially along the length of the arc column. In the main nozzle the temperature near the nozzle surface can be well above 4000 K and the radial temperature profile in the space between the two nozzles can become non-monotonic during the high current phase. Thus in the present work, the radiation radius for the calculation of radiation emission is defined as the radial distance from the axis to the isotherm of $0.83T_m$ in the high current phase (from arc initiation to the point of 15 kA magnitude before the final current zero) and the average of the two radii corresponding to $0.83T_m$ and 5000 K in the current zero phase (from the end of the high current phase to the final current zero point). The use of the above two methods to define the radiation radius gives nearly identical radial temperature profiles while preventing numerical difficulties in the simulation. More details of the radiation model can be found in [1] and [6]. The NEC data given in [7] is multiplied by a factor of 1.5, which produces reasonable arc voltage in the high current phase.

Radiation is emitted from the arc core. Once the volumetric radiation energy source is calculated, the total radiative flux from the arc core can be obtained by volume integration. 50% of this radiation flux is assumed to be absorbed at the arc edge. The distribution of the negative volumetric energy source as a result of radiation re-absorption in the region from R_{83} to R_{5K} as a function of radius is given by:

$$q_a(r) = q_0[1.1 - (\frac{R_{5K}+R_{83}-2r}{R_{5K}-R_{83}})^2]$$
(2)

where R_{83} and R_{5K} is the radius at $0.83T_{max}$ and 5000 K, respectively. q_0 is a constant that can be calculated from the following expression

$$q_0 = \frac{0.5Q_{core}}{\int_{R_{83}}^{R_{5K}}[1-(\frac{R_{5K}+R_{83}-2r}{R_{5K}-R_{83}})^2]2\pi r dr}$$
(3)

where Q_{core} is the total radiation flux from the arc core. The other 50% of Q_{core} reaches the nozzle wall producing nozzle ablation.

The effect of nozzle ablation is considered by solving a mass concentration equation for PTFE vapour. The amount of PTFE vapour injected into the flow domain is obtained by [9]

$$\bar{m} = \frac{Q_{noz}}{h_v}$$
(4)

where Q_{noz} is the radiation flux per unit axial length reaching the nozzle surface, $\bar{m}$ the rate of ablation per unit length as a mass source injected into the flow domain, and h_v the energy required to break up the PTFE polymer chain and to raise the PTFE vapour from 300 K to 3400 K [10], which is equal to 1.19×10^7 J/kg.

The electrical power input and current density is calculated by solving the current continuity equation in the high current phase. The use of transparent contacts and arc roots was explained in [1] [3] for, respectively, the continuity of current and ensuring reasonable size of the arc roots in a two dimensional axisymmetric model. The current continuity equation is solved in an enlarged domain with which the

electric field and current density inside and near the arc column are not sensitive to the conditions imposed on the boundary of the computational domain where $\frac{\partial \varphi}{\partial n} = 0$ is specified [1], φ is the electrostatic potential. The potential on the end of the live contact intersecting with the computational domain boundary is set to zero. A uniform current density is specified in a circular area on the tip of the transparent contact which is located inside the hollow contact. The radius of this circular area is determined by the instantaneous current and a uniform current density of 1.5×10^8 A/m^2 based on experimental evidence. This approach provides computational stability and the predicted arc voltage matches the measurement well [3]. The magnetic flux density has a dominant azimuthal component which is calculated by Ampere's circuital law [11]. The valves used in circuit breakers consist normally of a valve plate, a base plate and auxiliary springs. The operation of the valves is simplified in the simulation. The opening and closing of valves are approximated by unblocking and blocking the holes in the base plate in response to the pressure difference on both sides of the valve holes [12] (black region shown in Fig. 1).

Prantl mixing length model is used. The turbulent viscosity is given by

$$\mu_t = \rho {l_m}^2 \sqrt{(\frac{\partial \omega}{\partial r})^2 + (\frac{\partial v}{\partial z})^2} \tag{5}$$

The length scale l_m for tubulent momentum transport is expressed as the product of the arc thermal radius and a turbulence parameter

$$l_m = c \cdot R_{arc} \tag{6}$$

where Rarc is defined as the radius of 5,000 K isotherm in the high current phase and 3,000 K isotherm in the current zero phase. The coefficient c is set to be 0.05 for the high current phase, and linearly changed with the magnitude of current between 0.05 and 0.3 in the current zero phase [3]. For post arc current calculations c is fixed at 0.3. The choice of 0.3 is reasonable, it is a result of calibration between measured and predicted arc voltage at low current levels and by type test results where thermal interruption succeeded in one case and failed in another case with similar switching conditions. Real test conditions including the current and contact travel are used for the simulation.

The flow computational domain is shown in Fig. 1. The circuit breaker is initially filled with SF6 at an absolute pressure of 0.6 MPa at 300 K. Axisymmetric boundary conditions are applied for all solved for variables on the axis. The normal gradient of all solved for flow variables are set at zero on the boundary. The pressure at the two exits, which are indicated by the parallel arrows in Fig. 1, is fixed at 0.6 MPa.
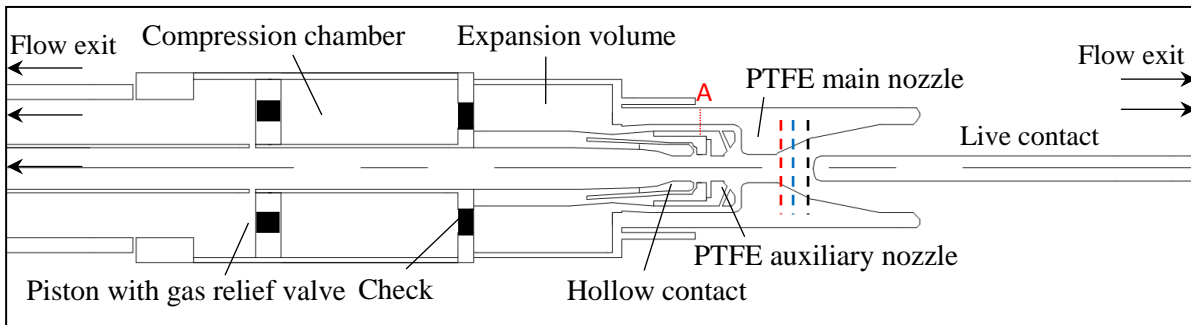
Figure 1. Simplified geometry and computational domain of the 145 kV auto-expansion circuit breaker under investigation. The final position of the live contact is shown by the three dash lines near the live contact tip for different arc durations.

3. Results and discussion
The model has been used previously to predict the pressure rise in auto-expansion circuit breakers [5] and arc voltage in a puffer circuit breaker [3], producing results matching reasonably well with measurement. The circuit breaker (Fig. 1) is rated at 145 kV and 40 kA with a power frequency of 60Hz. The arc is initiated in simulation when the contacts separate at a distance of 8 mm at 12.72 ms. The short, medium and long arc durations are 12.25 ms, 15.25 ms and 18.62 ms (from arc initialization to current zero) based on the type test results. The initial current is set to 3 kA and ramps up in 0.3 ms to the instantaneous value to start the arc and avoid computational difficulties. The influence of this artificial current ramping has been studied and its influence is restricted to the first millisecond, thus its impact on the high current phase in terms of nozzle ablation and pressure built-up in the expansion volume can be safely ignored.

3.1 Comparison of pressurization in the expansion volume
Fig. 2 shows the pressure variation in the expansion volume for different arc durations with identical peak values of the current. Before the live contact clears the tip of the auxiliary nozzle (tip position is indicated by Position a in Fig. 4) at 16.5 ms, the relatively low rise of pressure (0.05 MPa from 12.7 ms to 16.5 ms) in the expansion volume for all three cases is mainly caused by the puffer action leading to gas compression. The arc is effectively isolated from the main nozzle and the heating channel (the annular channel connecting the nozzle and the expansion volume) by the live contact. The maximum pressure in the hollow contact shortly before 16.5 ms is around 10.6, 2.0 and 2.4 MPa for short, medium and long arc durations, respectively.

The hot gas inside the hollow contact rushes towards the heating channel when the live contact clears the auxiliary nozzle. However this process is not expected to lead to significant pressure rise in the expansion volume at the initial arcing stage because of the small volume of the hollow contact hole. As it was found in [12], pressurization in the expansion volume is closely associated with the thermal energy flux into it. This is shown in Fig. 3. The enthalpy flux depends on two factors, i.e. the area of PTFE surface exposed to radiation and the magnitude of the instantaneous current flowing through the arc.

The long arc duration case has the earliest enthalpy flux (recorded at location A of Fig. 1) increase at 16.5 ms into the expansion volume because of the increasing arcing current approaching its first peak located at 17.8 ms. It has a higher enthalpy flux than the short arc duration case because of the difference in the instantaneous current, leading to different level of ablation in the auxiliary nozzle. As a result, it has a high pressure rise in the expansion volume at the initial stage up to 19 ms for the long arc duration case. However, the enthalpy flux starts to drop soon after the current passes its first peak. Gas pumping completely stops at 20. 7 ms when the current falls to 16 kA, which is evidenced by the zero enthalpy flux towards the expansion volume in Fig. 3. During this period (before 20.7 ms) the arc is mainly burning in the auxiliary nozzle and space between the auxiliary nozzle and the main nozzle (Fig. 4a). The arc column is less confined in space and the radiation flux reaching the ablation surface is moderate (10^3 MW/m^2), which explains the lower enthalpy flow rate (-5 MJ/s) in comparison with the second half cycle of the long arc duration case (-15MJ/s).

When the live contact tip moves through the flat throat of the main nozzle (distance between position b and c in Fig. 4), the current approaches its zero point and there is virtually little ablation generated. A reverse flow period (from 20.7 to 22.8 ms) then occurs until the current reaches 20 kA in the second half cycle at 22.8 ms. At this time the arc burns in a considerable length of the flat throat of the main nozzle, exposed to much more ablating surface. In addition, the current goes through its peak of 56 kA, generating a much higher enthalpy flow rate (- 15 MJ/s) into the expansion volume. The pressure in the expansion volume also increases from 1.5 MPa to over 4.0 MPa in 5 ms (from 24 ms to 29 ms) before it drops to 3.8 MPa at current zero.

For medium arc duration, the enthalpy flow rate also increases (to -0.6 MJ/s) after 16.5ms, but lasts for a very short time (less than 0.5 ms), and then drops because the current is rapidly approaching its zero point before 18.3 ms. At 19.5 ms with an instantaneous current of 20 kA, the enthalpy rate begins to rise again. This indicates that 20 kA is a threshold current for the formation of an ablation dominated arc in the given configuration. In addition, from 19.5 to 23 ms (current peak), the live contact travels through the full length of the flat throat of the main nozzle. Due to the high current during this period, PTFE is effectively ablated which significantly increases the enthalpy flow rate to -18 MJ/s (Fig. 3). Therefore, the pressure rapidly increases to the peak of 4.1 MPa at 3 ms after the current peak because it takes time for the contact gap to be pressurized and then thermal energy is convected into the expansion volume.

As expected, the enthalpy flow rate in the short arc duration case experiences a delayed rise (Fig. 3) between 17 ms and 18 ms in comparison with the long arc duration case because of the lower current level shortly before the live contact clears the auxiliary nozzle. The current already starts to drop after its positive peak when the tip of the live contact moves into the flat throat of the main nozzle around 20 ms. Its enthalpy flow rate into the expansion volume carries increasing after the current peak until 21.5 ms because the flat throat of the main nozzle is still blocked by the live contact, which is different from the other two cases. The final position of the live contact tip at current zero is just out of the exit of the main nozzle throat (see Fig. 1). Since in the high current phase the main nozzle is blocked by the live contact and ablation in the auxiliary nozzle creates a stagnant region, vapour compression in the main nozzle rapidly establish a high pressure zone and develops a high enthalpy flux (-17 MJ/s) towards the expansion volume (Fig. 3).

For the geometry under investigation which is representative of modern auto-expansion circuit breakers, the final half-cycle of the current is mainly responsible for the pressurization in the expansion volume. In particular in the long arc duration case, the final half-cycle produces 77% of the total pressure rise in the expansion volume. While the fluctuation on the pressure curve is due to change in arc column size generating pressure waves propagating towards the expansion volume, the overall delay is caused by the development of the high pressure zone in the contact space and the motion of hot vapor across the length of the heating channel into the expansion volume.

The delay between the current peak and the pressure peak in the expansion volume is respectively, 3.4, 2.9 and 3.2 ms for the short, medium and long arc duration cases. It is interesting to note that auto-expansion circuit breakers with overall different designs have very similar values for the delay between the last current peak and the last pressure peak in the expansion volume, with an average value of 3±0.2 ms. Attempts have been made to identify the causes for this rather constant value of time delay. The length of the heating channel is 100 mm. It was found that the time taken for pressure to propagate from the contact space to the expansion volume is only a small fraction (~0.2 ms) of a millisecond.

Taking the short arc duration case as an example, pressure recorded at different positions (P1-P4 as shown in Fig. 6) in the arcing chamber show that this delay consists of two stages, as shown in Fig. 5a. The first stage (20 ms to 21.7 ms) is designated by rapid pressurization of the expansion volume when large pressure difference between expansion volume and nozzle throat exits. At 21.7 ms the pressures at P2 (in the heating channel) and P1 (in the expansion volume) reach the same level. In the second stage (21.7 ms to 23.4 ms) pressure at P3, the axially middle plane of the flat throat of the main nozzle, has reached a new height in its magnitude following vapour accumulation and flow field adjustment. This high pressure drives further enthalpy flux into the expansion volume. With the pressure difference between the contact space and the expansion volume becoming smaller, the rate of rise of pressure also decreases until an instant (around 23.4 ms) the pressure difference becomes zero and pressurization vanishes. The use of a flat throated main nozzle and auxiliary nozzle of similar structure and comparable dimensions in modern auto-expansion circuit breakers (31.5 kA to 40 kA, 145 kV to 252 kV) gives the rather similar values in
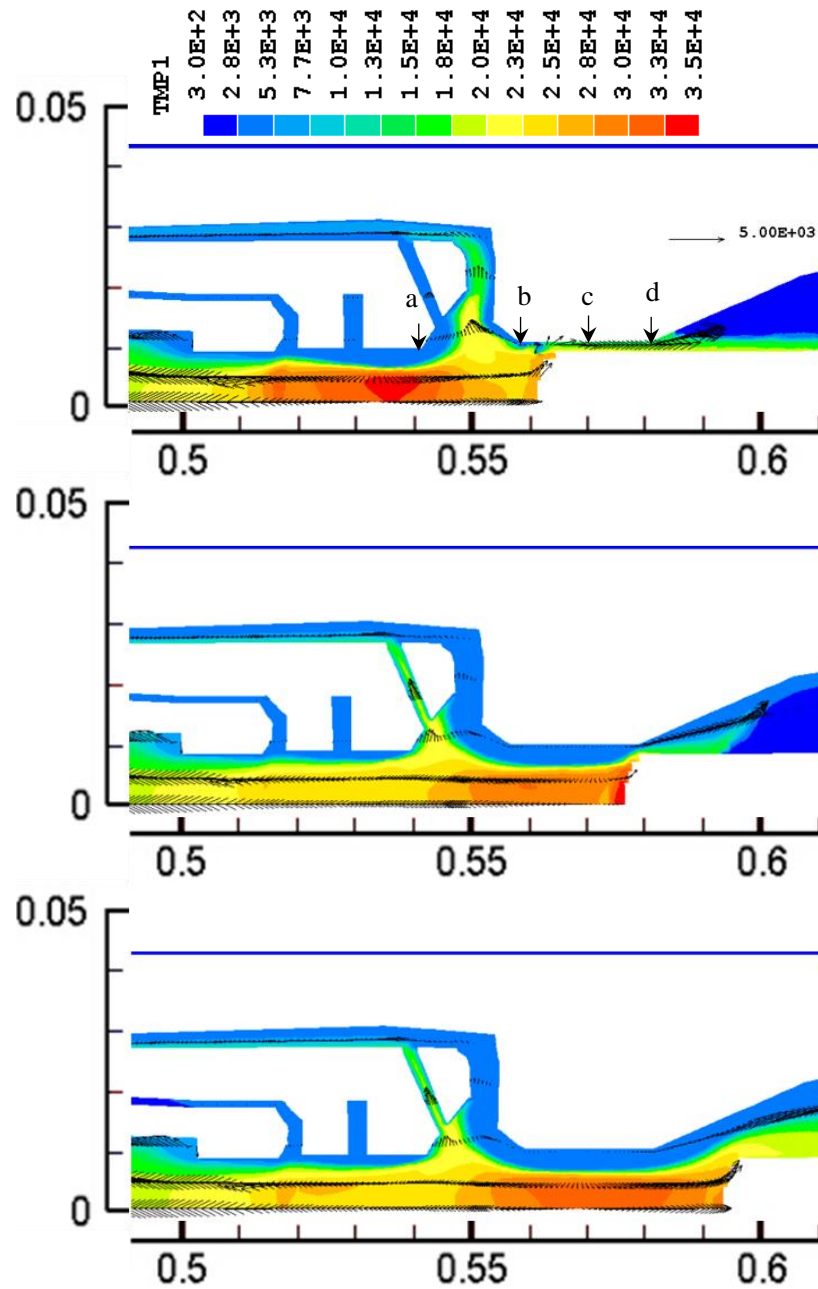
this time delay [1][12][13][14]. The other two cases shown in Fig. 5 follow similar pattern of pressure variation and will not be repeated in detail.
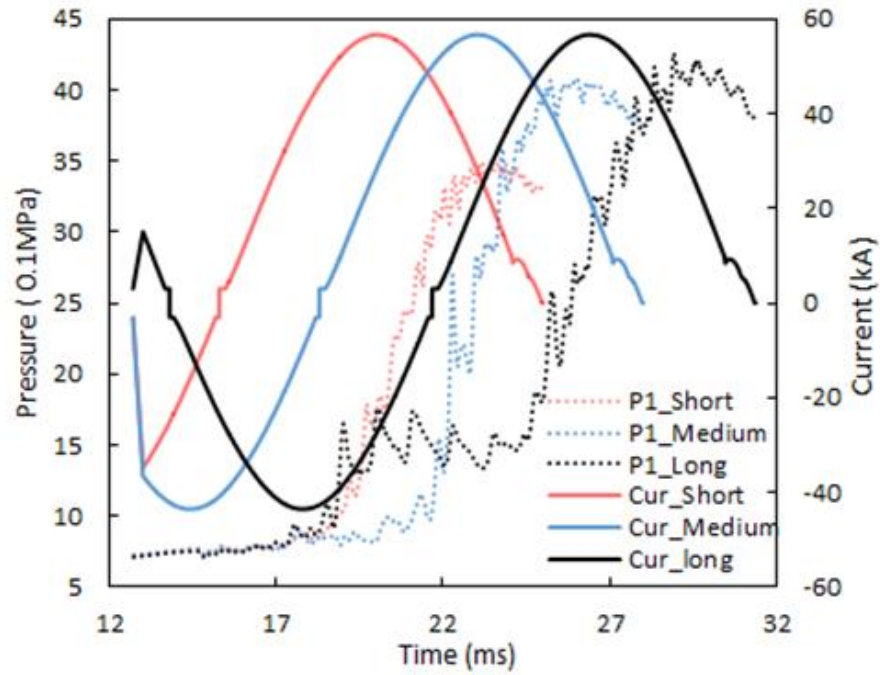
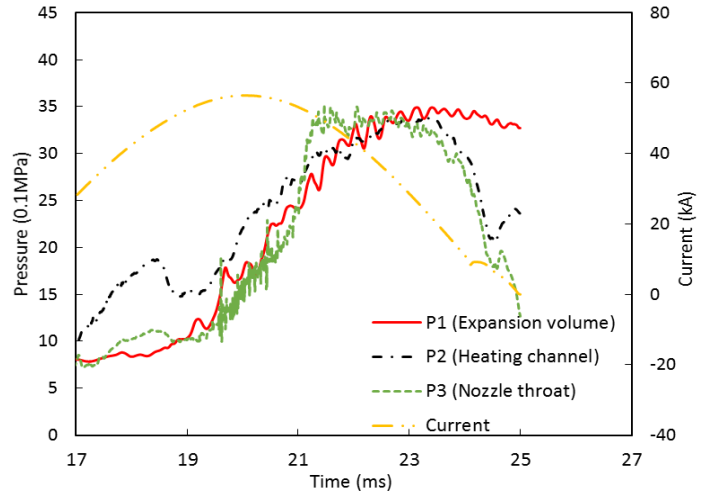**Figure 2.** Predicted pressure rise in the expansion volume.
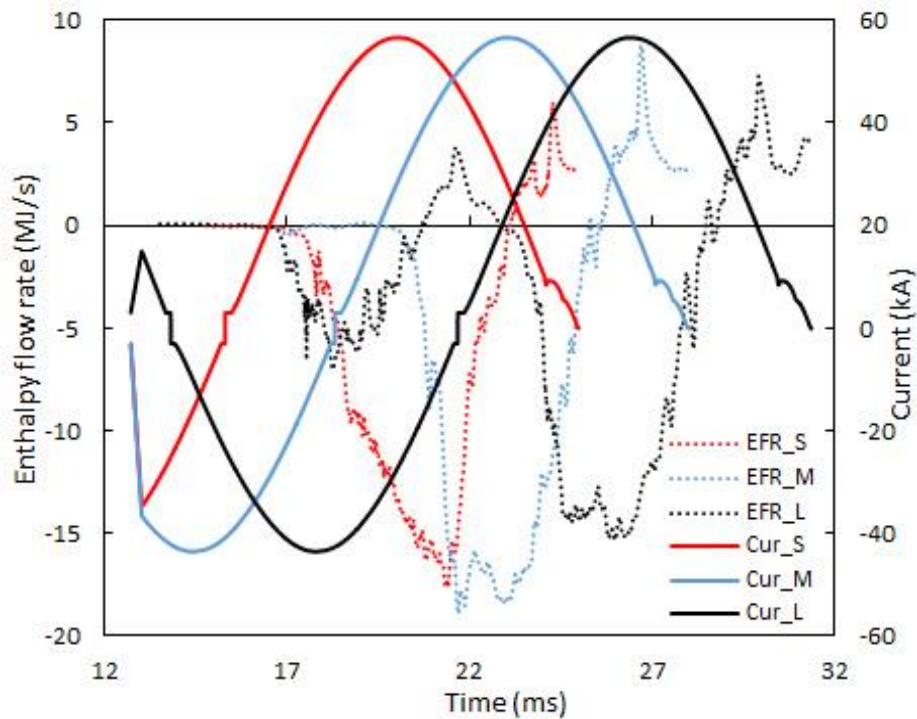
Figure 3. Enthalpy flow rate at location A in Fig. 1 in the heating channel at high current phase.
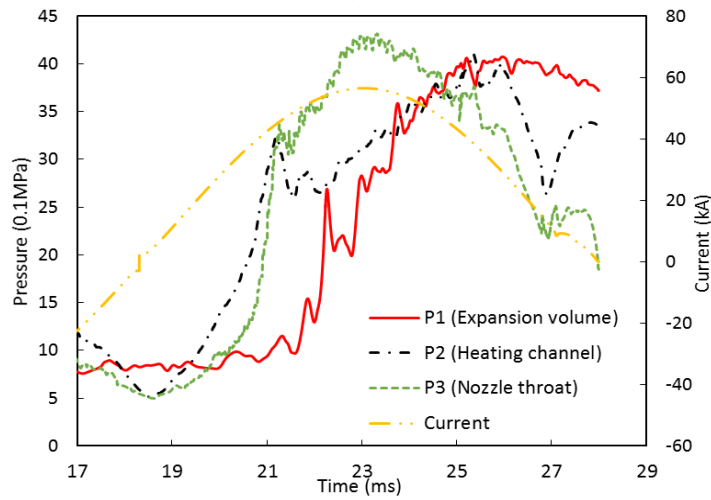
Figure 4. Temperature distribution with velocity field for short, medium and long arc duration at current peak of 56 kA from top to bottom, the time instant for live contact position is (a) 16.5ms (b) 19.5ms (c) 21.3ms (d) 23.5ms.

(a)

(b)
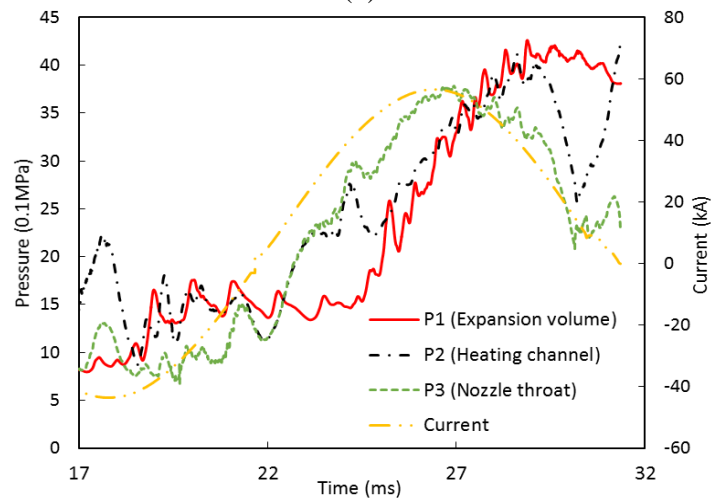
(c)

Figure 5. Pressure records in the arcing chamber for (a) short (b) medium, and (c) long arc duration.
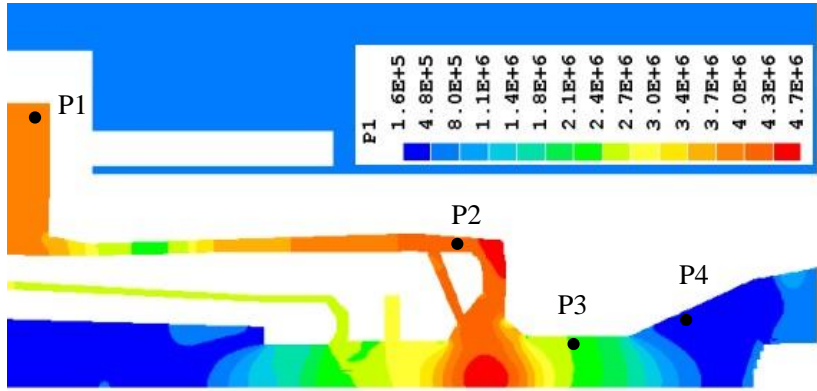
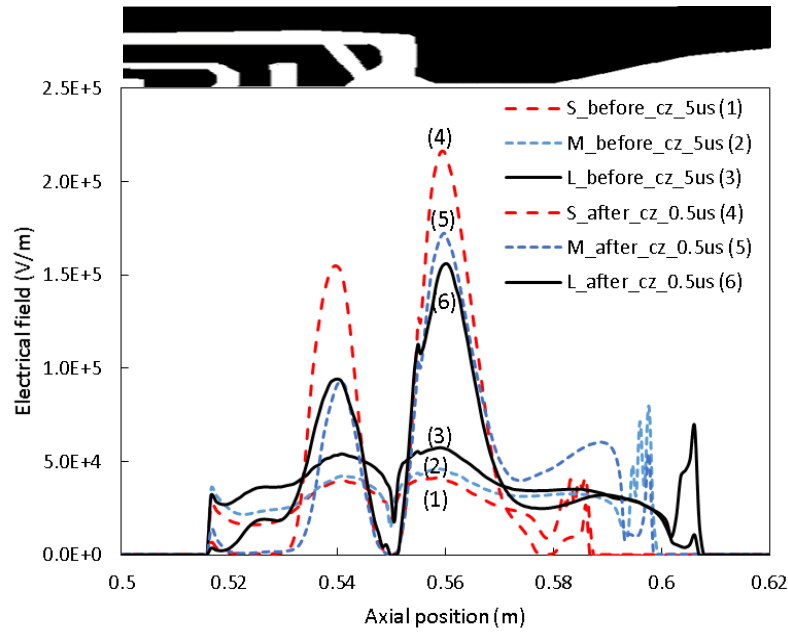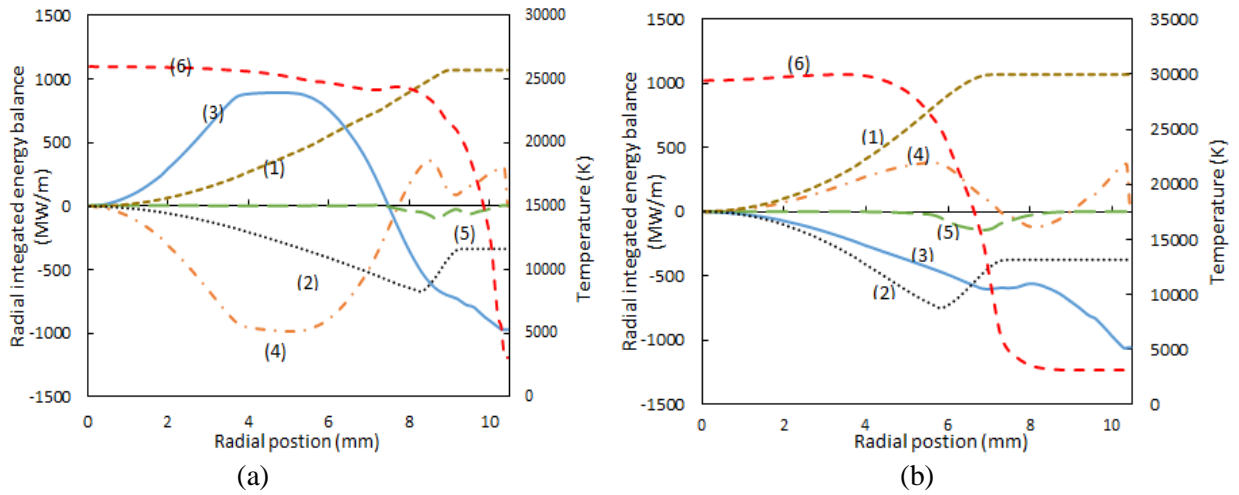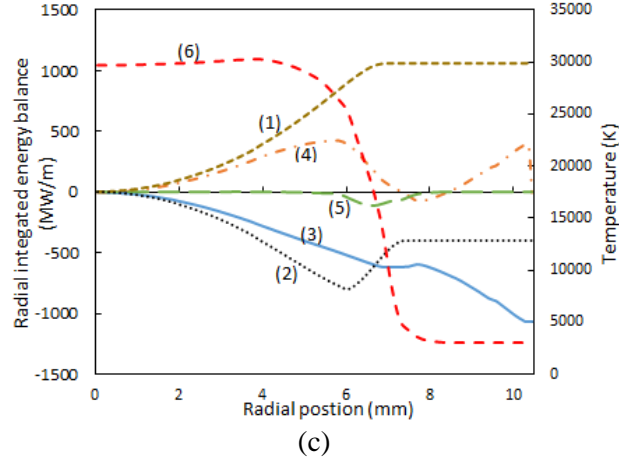**Figure 6**. Pressure distribution for long arc duration at current zero

Figure 7. Axis electrical field 5us before current zero and 0.5us after current zero under dv/dt of 8kV/μs.

(a)

(b)

(c)

Figure 8. Radial integrated energy balance of critical cross section with axial position 0.55 m at final current peak for (a) short (b) medium and (c) long arc duration. The curves present

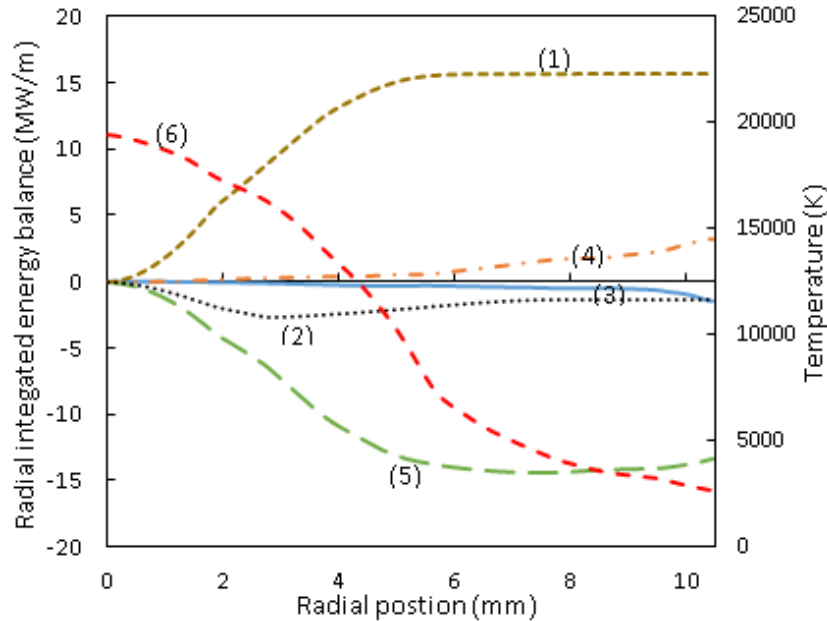(1) Ohmic heating: $\int \sigma E^2 2\pi r dr$

(2) Radiation loss: $-\int q 2\pi r dr$

(3) Axial convection: $-\int \frac{\partial}{\partial z}(\rho\omega h)2\pi r dr$

(4) Radial convection: $-\int \frac{1}{r}\frac{\partial}{\partial r}(r\rho vh)2\pi r dr$

(5) Radial thermal and turbulence conduction: $-\int \frac{1}{r}\frac{\partial}{\partial r}(-r\frac{k}{C_p}\frac{\partial h}{\partial r})2\pi r dr$

(6) Radial temperature profile

Figure 9. Radial integrated energy balance at 500A for the short arc duration case, the meaning of each curve is same as Fig.8.

3.2 Flow environment before current zero

The quality of arc quenching at current zero depends on the flow field around the arc column. Both velocity and density affects the interruption process. From Fig. 7, the region around an axial position of

0.56 m (corresponding to the left end of flat nozzle throat) and the region inside the auxiliary nozzle take up a considerable part of the recovery voltage. This means the arc temperature decays most rapidly in these two regions and arc resistance recovers to high values. In order to track the causes, energy balance is performed at the axial location of 0.56 m to identify the dominant energy transport mechanisms at several key instants before current zero.

Depending on the local flow field, energy transport at high current behaves differently from the low current arcs. For the short arc duration case at its peak current, convection dominates the energy transport process (curve (3) and curve (4) in Fig. 8a). This is because at this instant the location for energy balance is close to the tip of the live contact, and energy is convected into the domain in the positive axial direction and convected out in the positive radial direction. For both medium and long arc duration cases, the live contact at peak currents has cleared the flat nozzle throat and strong axial flow been established (Fig. 8b and 8c). The net effect of axial convection on energy balance in the arc core becomes weaker. Ohmic heating and radiation dominate the energy transport process (curve (1) and (2) in Fig. 8b and 8c). Approaching current zero, turbulence plays an increasingly important role. At 12 kA, the arc changes from radiation dominated to turbulent cooling dominated, turbulence cooling overtakes other mechanisms. At 500 A (30 μs before current zero) turbulent cooling is the dominant mechanism for energy removal (curve 5 Fig. 9).

Results in Fig. 10 clearly show that at the current zero point, the axis temperature in the long arc duration case is the lowest and that of the medium arc duration case behaves similarly but is 300 K higher. In the short arc duration case the flat throat of the main nozzle is still partially blocked by the live contact and the arc column is larger, leading to a higher temperature near the nozzle wall. Cooling of the arc by the surrounding axial flow in the current zero period is a combined effect of gas velocity and density, determining the mass flow rate. Fig. 11 shows that the axial mass flux of the surrounding gas flow is rather uniform in the majority part of the nozzle cross section (from a radius of 2.5 mm to 8 mm). The long arc duration case has the highest value of 1.64×10^4 kg/m^2/s, which is 2.7 and 2 times higher than that of the short and medium arc duration cases, respectively. The arc column of the long arc duration case is thus thinnest in comparison with the other two cases (Fig. 12). When the current reaches its zero point pressure drop in the auto-expansion volume from its peak value is normally within 10% of the maximum pressure rise (pressure peak minus the filling pressure) as shown in Fig. 2.

A stronger flow (mass flow rate) from the expansion volume towards the nozzles is designated by a lower pressure difference between the expansion volume and the middle position of the flat nozzle throat (P3 in Fig. 6), or a higher pressure difference between the heating channel (P2) and exit (P4) of the flat nozzle throat, as given in Fig. 13. The main cause for this relationship is due to the fact that the pressure in the heating channel (P2) starts to recover shortly before current zero, at 24.6 ms, 26.95 ms, 30.22 ms for short, medium and long arc duration cases (details see Fig. 5). Due to pressure reflection by the bent solid surface near P2, the pressure at P2 can become higher than that in the expansion volume (Fig. 5c). The pressure distribution for the long arc duration case has been given in Fig. 6. It is this recovered pressure in the heating channel that supports the flow field and thus the mass flow rate near current zero.

For Fig.5c it should be noted that because the tip of the live contact clears the main nozzle throat before the current reaches its peak, the maximum pressure in the contact space is not at the middle of the nozzle throat in the pressurization stage. Instead the maximum pressure is close to the upstream end of the flat nozzle throat, which is responsible for pumping hot vapour into the expansion volume and raise the pressure to 4 MPa.
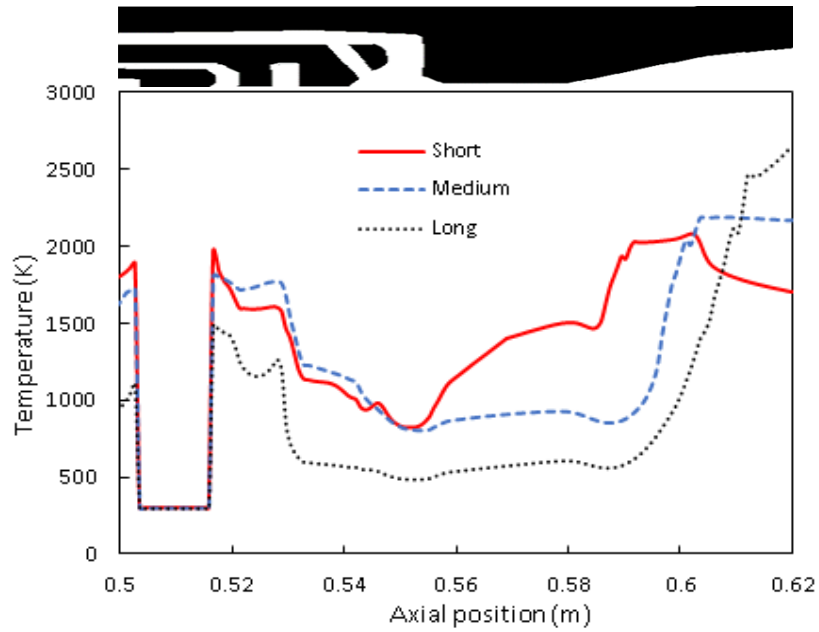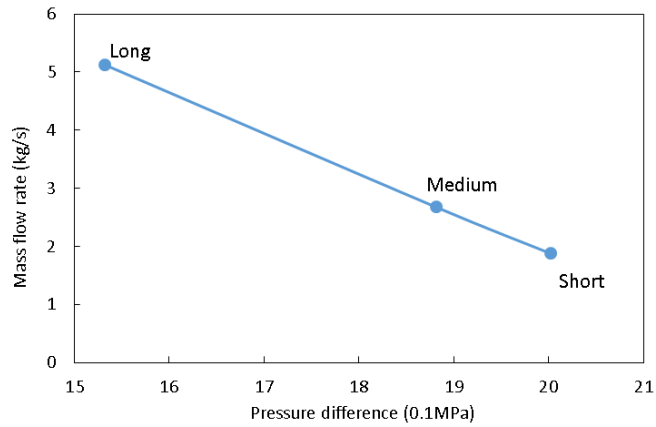
Figure 10. Temperature at current zero along an axial line that is 1mm away from the nozzle surface
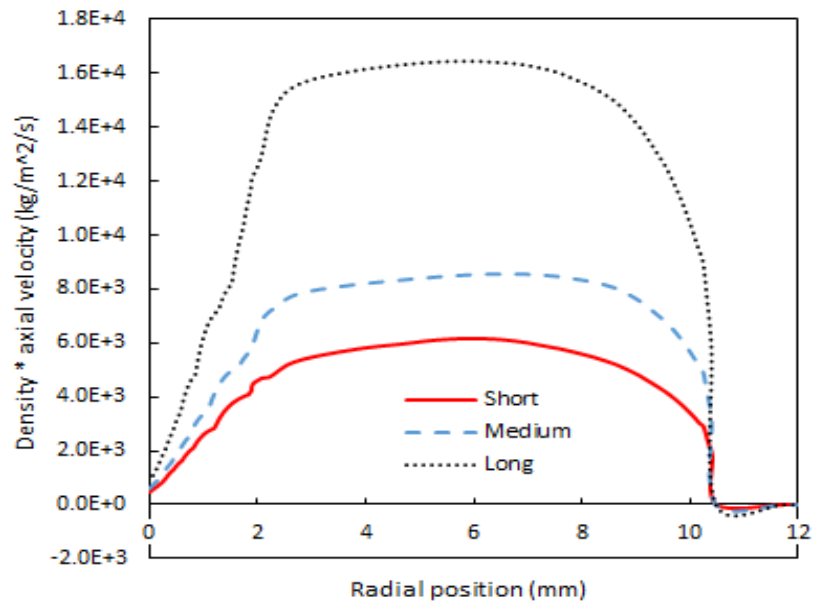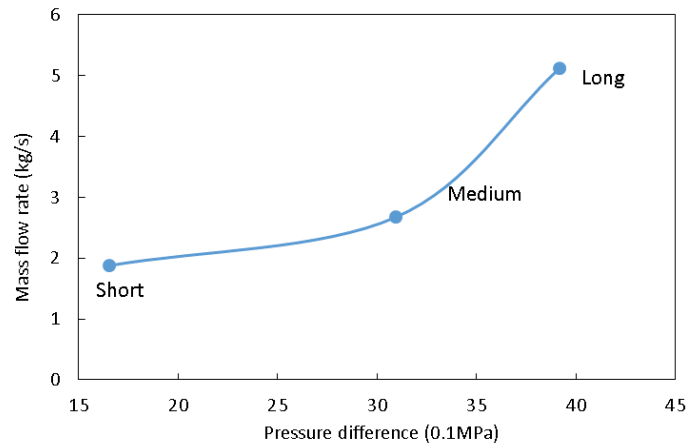

Figure 11. Radial mass flux distribution at the axial position of 0.56 m at current zero.
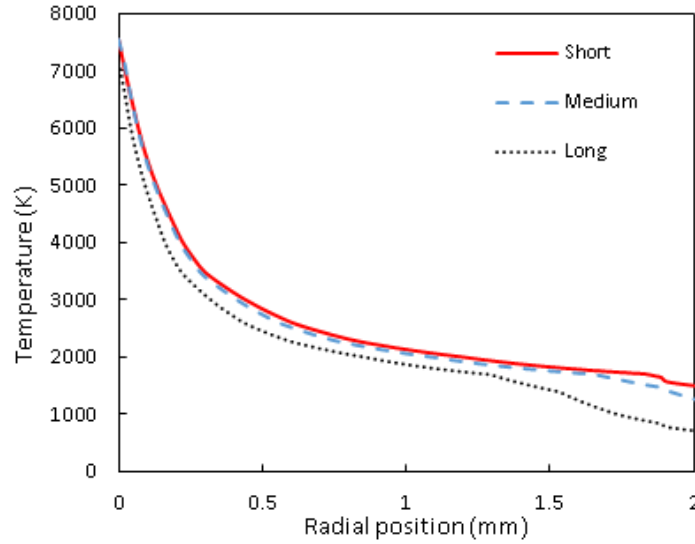
Figure 12. Radial temperature distribution at the axial position of 0.56 m at current zero.
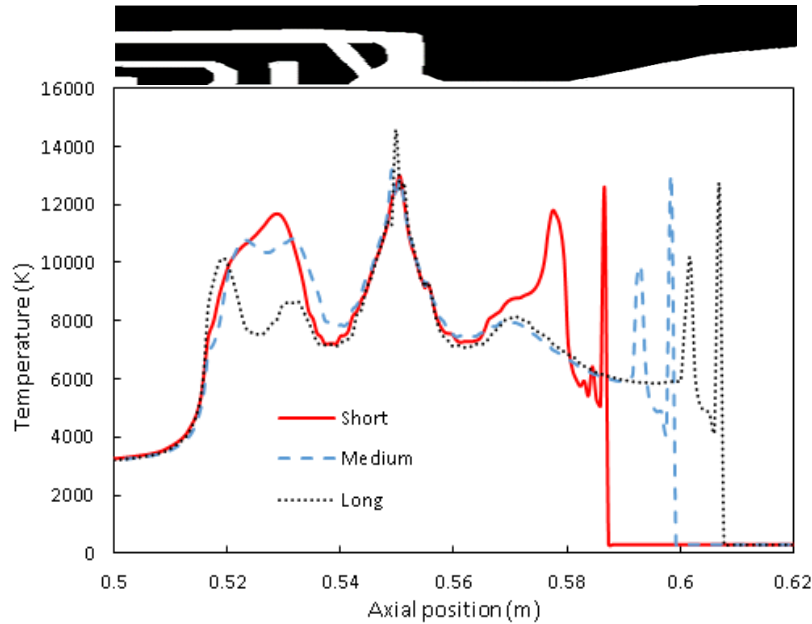

(a)

(b)

Figure 13. Mass flow rate at the axial position of 0.56 m versus pressure difference between (a) expansion volume and the middle of nozzle throat, i.e. P1-P3 in Fig. 6; (b) heating channel and downstream of nozzle throat at current zero, i.e. P2-P4 in Fig. 6.

Figure 14. Axis temperature for different arc durations at current zero.

Turbulence enhanced momentum and energy transfer is most significant in the current zero phase of high voltage circuit breakers. Recently there is qualitative evidence that turbulence also contributes to the mixing of hot and cold gases in the expansion volume [16][17]. In the present work, a very small turbulence mixing length scale is used in the expansion volume of the breaker due to a lack of reliable information on the strength of turbulence mixing effect. The expansion volume is relatively long in comparison with its radial extent and hot gas flows towards the bottom of the expansion volume in the pressurization stage. It is well known that pressure rise in the expansion volume depends mainly on the energy flow rate into it, not the mixing of the gas. Our results show that gas temperature in the expansion volume after flow reversal is generally lower than 2000 K. It is not expected that any possible turbulent mixing of gas in the expansion volume would affect the results significantly in the present work.

3.3 Thermal recovery process
Fig. 14 show that closely associated with the surrounding gas flow, arc temperature on the axis has two valleys after current zero, one near the tip of the auxiliary nozzle (axial position of 0.54 m) and the other near the left end of the flat throat of the main nozzle (axial position of 0.56 m). The arc temperature in the main nozzle for the short arc duration case remains above 8000 K, different from the other cases. Results in Fig. 7 and 15 provide evidence that for the short arc duration case recovery voltage from the system has to be taken up by the gas in the auxiliary nozzle and a small section of the gas in the main nozzle. A comparison of voltage share for the three cases is given in Table 2. The current is 98 A at 5μs before the final current zero. It is clear that
a) The gas in the auxiliary nozzle region takes about 40% of the arc voltage shortly before the final current zero and in the short arc duration case this figure is 46% because of the relatively shorter contact gap;
b) Arc in the main nozzle is more rapidly cooled down to take an increased share of the recovery voltage after current zero (> 65%);
c) In the short arc duration case the auxiliary nozzle region plays a more important role in the thermal recovery process in comparison with the other two cases.

At current zero a hot spot is formed in front of the live contact in all cases. This is due to the arc flow hitting the contact tip surface and causing a stagnation region with possible reverse flow (Fig. 16). As a design guidance, the shortest arc duration for successful thermal interruption is achieved when the ring shaped flow cross sectional area between the tip of the live contact and the main nozzle equates the value of the nozzle throat cross section area shortly before the current zero point in the course of contact motion. At that moment, the circuit breaker is considered to establish adequate interruption ability because there is sufficiently large flow area to develop the gas flow at current zero. Comparing the flow field of three switching duties in Fig. 16, the velocity in the short arc duration case is much lower than the other two cases because the blocking effect of the live contact. As a result, strong convection and turbulent cooling cannot be established in the main nozzle at current zero for the short arc duration case.

Table 2. Voltage across two sections of arc column separated by the stagnation point.

Case		Auxiliary nozzle (V/%)		Main nozzle (V)	Total voltage (V)
5us before C.Z.	Short	936	46.3	1085	2021
	Medium	1071	38.3	1725	2797
	Long	1402	39.2	2172	3575
0.5us after C.Z.	Short	1432	35.8	2568	4000
	Medium	789	19.7	3211	4000
	Long	1208	34.0	2793	4000

3.4 Critical rate of rise of recovery voltage (RRRV)

The critical RRRV of a circuit breaker is a direct indicator of its interruption capability. It is a threshold value of dv/dt (or RRRV applied across the contact gap after current zero). Any dv/dt that is higher than this threshold value will eventually lead to thermal re-ignition. Computationally, for a specified set of arcing conditions, different dv/dt values are used to calculate the post arc current as a function of time. There will be two dv/dt values, one leading to thermal re-ignition and the other one leading to thermal recovery. The average of these two values can then be regarded as the critical RRRV.

The initial RRRV imposed by the network during a short line fault (SLF) is considerably higher than that during a terminal fault. In a 40 kA and 60 Hz scenario, the value of dv/dt is around 9 kV/μs in the first 2 microseconds, as evidenced in type test records and also in literature [18]. To investigate the variation in interruption capability, the critical RRRV is calculated for different arc duration cases after current zero. The computational uncertainty is less than 0.5 kV/μs.

At 5μs before the final current zero point, the arc has the higher axis temperature in the long arc duration case (Fig. 15). However, the temperature drops more rapidly after current zero leading to the lowest axis temperature at 0.5 μs after current zero, in comparison with those of the other two cases at the same axial position. This is a direct consequence of the strongest mass flux given in Fig. 11. The turbulent eddy viscosity at current zero is shown in Fig. 17 at two axial positions of 0.54 m and 0.56 m, respectively. It is evident that turbulent cooling is strongest in the long arc duration case. Its critical RRRV is thus expected to be the highest. The circuit breaker under investigation successfully passed all test duties. The predicted critical RRRV using a turbulence parameter of 0.3 is 10 kV/μs, higher than the applied RRRV of 9.0 kV/μs. The critical RRRV for the medium and long arc duration cases are both higher than 12 kV/μs. Despite the uncertainty in the turbulence parameter, it appears that a value of 0.3 produces a reasonable critical RRRV for the short arc duration case. The much higher critical RRRV for the other two cases indicates that this circuit breaker has a rather large margin in its interruption capabilities. It can also be argued that the short arc duration case is the most difficult switching duty for this type of auto-expansion circuit breaker and one of the design focuses should be with the careful choice of the shape and dimension

of the auxiliary nozzle based on the consideration in section 3.3.

There is recognition that deviation from local thermal equilibrium (LTE) and local chemical equilibrium (LCE) exists in the current zero period due to the fact that the time constants of chemical reactions differ significantly and electrons cannot pass their energy gained from the electric field to heavy particles in an efficient way duration the short time scale. This problem has been investigated in several publications [19][20][21][22]. It has been indicated that consideration of the non LTE and non-LCE effect alone is not able to produce reasonable predictions for the critical RRRV values. On the other hand it can be argued that the existence of turbulence in SF_6 arcs enhances not only the mass, momentum and energy transport process, but also increases the rates of chemical reactions around current zero, in a way similar to turbulent combustion, to render the plasma state closer to LTE and LCE. These issues collectively form one of the key research topics in the future to achieve quantitative prediction of the interruption capability of high voltage circuit breakers.
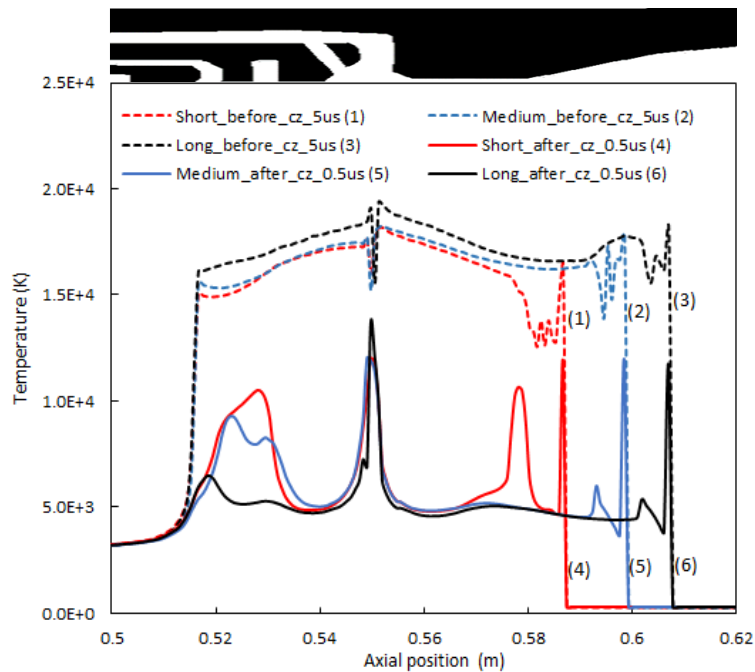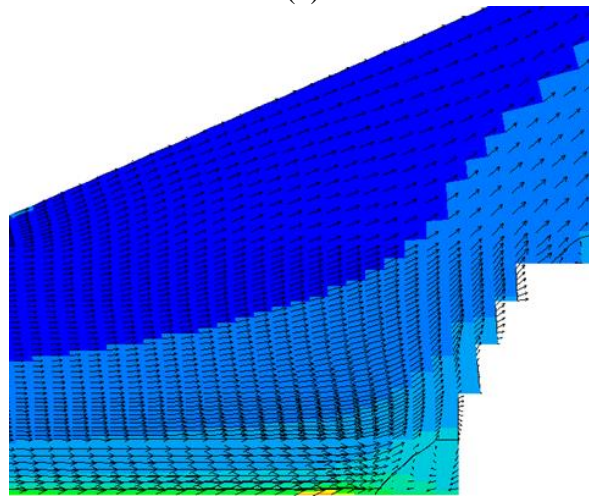

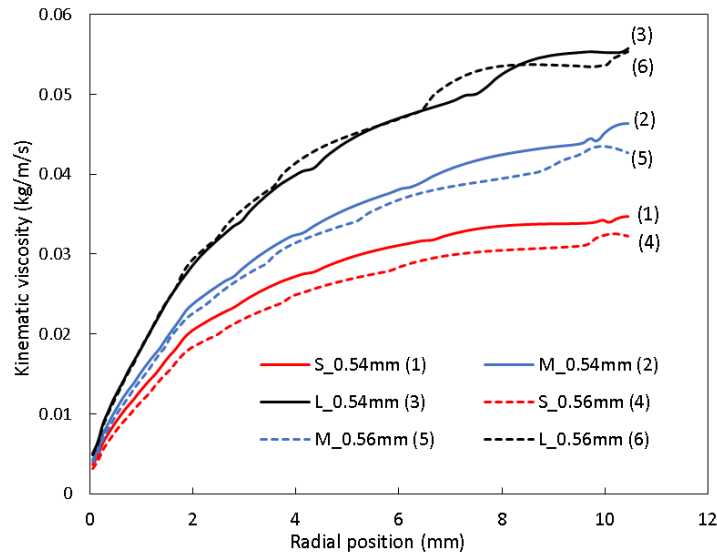**Figure 15.** Axis temperature 5 μs before current zero and 0.5 us after current zero under dv/dt of 8 kV/μs.
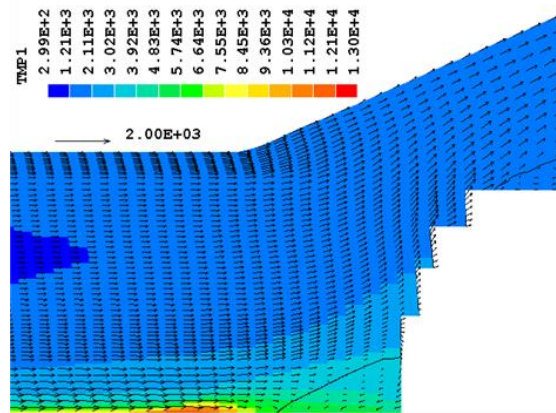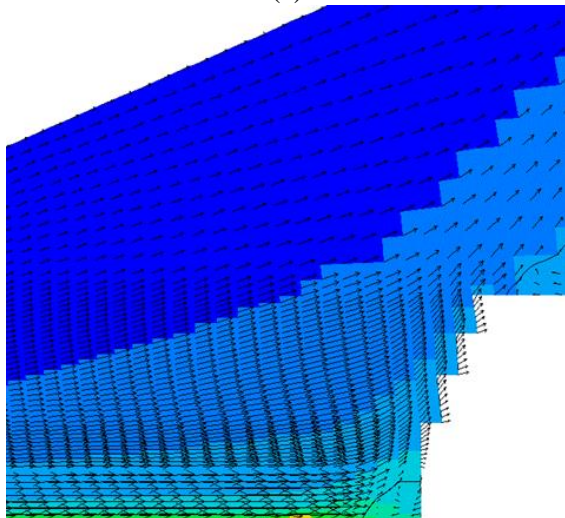
Figure 16. Temperature distribution with velocity field at current zero for (a) short, (b) medium and (c) long arc duration cases, respectively. The solid curve in front of the central part of the contact tip indicate zero velocity.

Figure 17. Turbulent eddy viscosity at the cross sections with axial position 0.54 m and 0.56 m for short, medium and long arc duration at current zero.

4. Conclusions

The behaviour of a 145 kV, 60 Hz auto-expansion circuit breaker with different arc durations and symmetrical short circuit current waveforms is computationally studied. The value of the turbulence parameter, which is key to quantitative prediction of the thermal interruption capability of gas blast circuit breakers, is carefully selected based on type test results.

a) The final half-cycle of the current is mainly responsible for the pressure rise in the expansion volume (77% for the long arc duration case). The auxiliary nozzle plays an important role in the pressurization process by creating a stagnation zone inside its hole to force the pressure in the contact gap to rise rapidly providing an enthalpy flux into the expansion volume. The peak enthalpy flow rate into the expansion volume is 17 MJ/s, 18 MJ/s and 14 MJ/s for short, medium and long arc duration cases, respectively. The pressure drop in the expansion volume from its peak value is within 10% when the current reaches its final zero point, implying that only a small fraction of the heated gas in the expansion volume flows out to establish the necessary flow field in the nozzles for arc quenching after current zero. The delay in time between the current and pressure peaks in the expansion volume is 3 ms, a rather constant value for different designs of auto-expansion circuit breakers.

b) When the current falls from its final peak toward the zero point the arc evolves from radiation and convection dominated cooling into a turbulent cooling dominated regime. The transition takes place at 12 kA. The increase in arc resistance is closely associated with the mass flow rate out of the expansion volume. At current zero the mass flow rate in the main nozzle is linearly related to the pressure drop over the heating channel. Due to the partial blockage of the main nozzle by the live contact, the arc column in the short arc duration case is hotter and larger in the main nozzle in comparison with the other two cases, leading to inferior interruption capability.

c) After current zero the system recovery voltage is shared by two sections of the contact gap divided by the flow stagnation point between the main nozzle and the auxiliary nozzle. The gas in the auxiliary nozzle region takes about 35% of the recovery voltage in the short arc duration case, which is the most difficult interruption duty of the three cases studied. It is evident that the auxiliary nozzle plays an

important part in both the pressurization process and the thermal recovery period, especially for short arc duration cases. Therefore, the dimension and location of the auxiliary nozzle should be a key technical consideration in the design of high voltage auto-expansion circuit breakers.

Acknowledgement

References

[1] Yan J D, Fang M T C and Hall W 1999 The development of PC based CAD tool for auto-expansion circuit breaker design *IEEE Trans. Power Delivery,* **14**, 176-81

[2] Park K Y and Fang M T C 1996 Mathematical modelling of SF6 puffer circuit breakers i: High current region *IEEE Trans on Plasma Sci.*, **24**, 490–502

[3] Yan J D, Han S M, Zhan Y Y, Zhao H F and Fang M T C 2009 Computer simulation of the arcing process in high voltage puffer circuit breakers with hollow contacts, Proceedings of XVIIIth Symposium on Physics of Switching Arcs, Brno Czech Republic, 99-108

[4] Pei Y, Zhang Q, Yan J D, Fang M T C 2011 Intelligent computer simulation tools for HV circuit breakers and issues related to simulation, in Electric power equipment-switching technology (ICEPE-ST) 1ST international conference, Xi'an China, 435-439

[5] Zhang J L, Yan J D, Murphy A B, Hall W and Fang M T C 2005 Computational investigation of arc behaviour in an auto-expansion circuit breaker contaminated by ablated nozzle vapor *IEEE Trans. Plasma. Science*, **30**, 706-19

[6] Zhang J F Zhang, Fang M T C and Newland D B 1987 Theoretical investigation of a 2kA arc in a supersonic nozzle", *J. Phys. D: Appl. Phys.* **25**, 1197-204

[7] Liebermann R W and Lowke J J 1976 Radiation emission coefficients for sulfur hexafluoride arc plasmas *J. Quant. Spectrosc. Radiat. Transf.* **17**, 253-64

[8] Private communication with Professor Vladimir Aubrecht

[9] Bu W H, Fang M T C and Guo Z Y 1990 The behaviour of ablation-dominated DC nozzle arcs *J. Phy. D: Appl. Phys.* **23**, 175-183

[10] Ruchti C B and Niemyer L 1986 Ablation controlled arcs. *IEEE Trans. on Plasma Science*, **14**, 423–434, 1986.

[11]Zhang J L, Yan J D, and Fang M T C 2004, Electrode evaporation and its effect on thermal arc behaviour*, IEEE Trans. on Plasma Science*, **32**, 1352-1361

[12] Wong T M, Yan J D, Ye X, Abrahamsson J and Fang M T C 2007 Global Thermal and Aerodynamic Environment in High Voltage Auto-Expansion Circuit Breakers. Proceedings of XVII Symposium on Pysics of Switching Arc. Local Organisation Comiittee, Brno, 37-46

[13] Liau V K, Lee B Y, Song K D, and Park K Y 2007 Computational investigation of arcing phenomena in 245 kV hybrid circuit breaker *Japanese Journal of Applied Physics*, **46**, 1674 – 1679

[14] Zhang Q, Yan J D and Fang M T C 2012 Computer aided design studies of auto-expansion circuit breakers Proceedings of the XIX International Conference on Gas Discharges and Their Applications, Beijing, China, 82-85

[15] Franck C M and Seeger M 2006 Application of high current and current zero simulation of high voltage circuit breaker *Contrib. Plasma Phys.* **46**, 787-797

[16] Bini R, Basse N T and Seeger M 2011 Arc-induced turbulent mixing in an SF6 circuit breaker model, *J. Phys. D: Appl. Phys.* **44**, 25203–12

[17] Gonzalez J J, Freton P, Reichert F and Randrianarivao D 2012, Turbulence and magnetic field calculations in high-voltage circuit breakers, *IEEE Trans. on Plasma Science*, **40**, 936-944

[18] Alexander R W, Dufournet D, Internets: Transient recovery voltage (TRV) for high-voltage circuit breakers, [Online]. Available: http://webm.dsea.unipi.it/barsali/materiale/Dinamica%20e% 20Controllo%20SE/TutorialTRVAlexander-Dufournet.pdf

[19] Gonzalez J J, Girard R and Gleizes A 2000 Decay and post-arc phases of a SF6 arc plasma a thermal and chemical non-equilibrium model, *J. Phys. D: Appl. Phys.* **33**, 2759-2768

[20] Girard R, Belhaouari J B, Gonzalez J J and Gleizes A 1999 A two- temperature kinetic model of SF6 plasma, *J. Phys. D: Appl. Phys.* **32**, 2890-2901

[21] Belhaouari J B, Gonzalez J J and Gleizes A 1998 Simulation of a decaying Sf6 arc plasma: hydrodynamic and kinetic coupling study, *J. Phys. D: Appl. Phys.* **31** 1219–32

[22] Girard R, Gonzalez J J and Gleizes A 1999 Modelling of a two-temperature SF6 arc plasma during extinction *J. Phys. D: Appl. Phys.* **32** 1229–38